Sensors & Actuators: B. Chemical 321 (2020) 128587

Contents lists available at ScienceDirect

Sensors and Actuators B: Chemical

journal homepage: www.elsevier.com/locate/snb

Mixed potential type H_2S sensor based on stabilized zirconia and a Co_2SnO_4 sensing electrode for halitosis monitoring

Caileng Wang[a], Li Jiang[a], Jing Wang[a], Fangmeng Liu[a,*], Rui You[b], Siyuan Lv[a], Zijie Yang[a], Junming He[a], Ao Liu[a], Xu Yan[a], Chenguang Wang[a], Peng Sun[a], Xishuang Liang[a], Geyu Lu[a,*]

[a] State Key Laboratory of Integrated Optoelectronics, Key Laboratory of Advanced Gas Sensors, Jilin Province, College of Electronic Science and Engineering, Jilin University, 2699 Qianjin Street, Changchun, 130012, China
[b] Institute of Microelectronics, Peking University, Beijing, 100871, China

ARTICLE INFO

Keywords:
H_2S sensor
YSZ
Co_2SnO_4 sensing electrode
Fast response time
Halitosis

ABSTRACT

An all-solid-state mixed potential type H_2S gas sensor was fabricated with yttria-stabilized zirconia (YSZ) solid electrolyte and Cobaltous stannate (Co_2SnO_4) sensing electrode (SE) for monitoring halitosis disease. The pure phase cubic spinel structure of Co_2SnO_4 prepared by simple hydrothermal method and annealed at 1000 °C was confirmed based on X-ray diffraction (XRD), Raman, Field-emission scanning electron microscopy (FESEM) and Transmission electron microscope (TEM) technologies. The developed sensor showed the lowest detection limit of 100 ppb, fast response/recovery time of 44/97 s and high sensitivity of -54.4 mV/decade to 0.1 – 10 ppm H_2S. The sensing device also gave good reproducibility, selectivity, humidity resistance and long-term stability. Finally, the simulated test for diagnosing halitosis was conducted and the evident difference of sensing response of the present sensor between healthy breath (collecting from healthy volunteers) and halitosis breath (healthy breath blended 1 ppm H_2S) indicated that the fabricated gas sensor using Co_2SnO_4-SE showed great potential application value in halitosis monitoring. The present work has opened up a new window to noninvasive and online diagnostics of halitosis in medical diagnosis and treatment.

1. Introduction

People with halitosis disease (i.e. oral malodour) may feel embarrassed in the conversation with others, which will lead to a lack of self-confidence and even affect their normal life. Besides, halitosis could be an omen of some underlying diseases such as gingivitis and periodontitis [1–3]. There have been some reports confirming that the halitosis of 80 %–90 % originated from the oral cavity, in which the sulphurcontaining amino acids cystine, cysteine, and methionine were decomposed into the foul-smelling volatile sulphur compounds (VSC), among which H_2S is one of the main productions [4–7]. In terms of the medical diagnosis, H_2S is used as a biomarker for halitosis. When the content of H_2S in human exhaled breath exceeds 0.1 ppm, it can be used as the basis for judging halitosis [4,8]. Therefore, the development of low-cost, portable and rapidly responsive H_2S gas sensors is of great significance for the early diagnosis and screening of halitosis.

In the last few decades, solid electrolyte type sensor has been proved to produce good consequences in detecting hazardous gases [9–13]. As for H_2S gas, Liang et al. reported a gas sensor of tubular structure based on sodium ionic conductor (NASICON) solid electrolyte and Pr_6O_{11}-doped SnO_2 sensing electrode, which had a sensitivity of 74 mV/decade to 5 – 50 ppm H_2S at 300 °C [14]. Zhang et al. found that the NASICON-based solid electrochemical sensor utilizing the $CoCr_{1.2}Mn_{0.8}O_4$ sintered with a temperature of 800 °C showed the highest response of 178 mV to 10 ppm H_2S at 250 °C [15]. However, due to the human exhaled breath contains large amounts of water vapour, the disadvantage of poor moisture resistance for NASICON-based sensors restricts their application in breath detection. Comparatively, the stabilized zirconia solid electrolyte type gas sensor based on mixed potential model showed enormous application potentiality due to better sensing stability. Miura et al. developed an electrochemical sensor combining Y_2O_3-stabilized solid electrolyte with WO_3 sensing oxide layer and found that the device responded well to 0.2 – 25 ppm H_2S at 400 °C [16]. Guan et al. designed a sub-ppm YSZ-based mixed potential type H_2S sensor using hollow ball $NiMn_2O_4$ sensing electrode, which showed highest sensitivity and lowest limit of detection of 50 ppb [17]. In addition, Lu's group used La_2NiO_4 as sensing electrode to fabricate YSZ-based sensor for H_2S detection, which could reach the detection limit of 20 ppb [18]. Even if above YSZ-based sensors have improved the sensitivity and lowered the detection limit, there still exist much space for

* Corresponding authors.
E-mail addresses: liufangmeng@jlu.edu.cn (F. Liu), lugy@jlu.edu.cn (G. Lu).

https://doi.org/10.1016/j.snb.2020.128587
Received 12 March 2020; Received in revised form 11 June 2020; Accepted 10 July 2020
Available online 13 July 2020

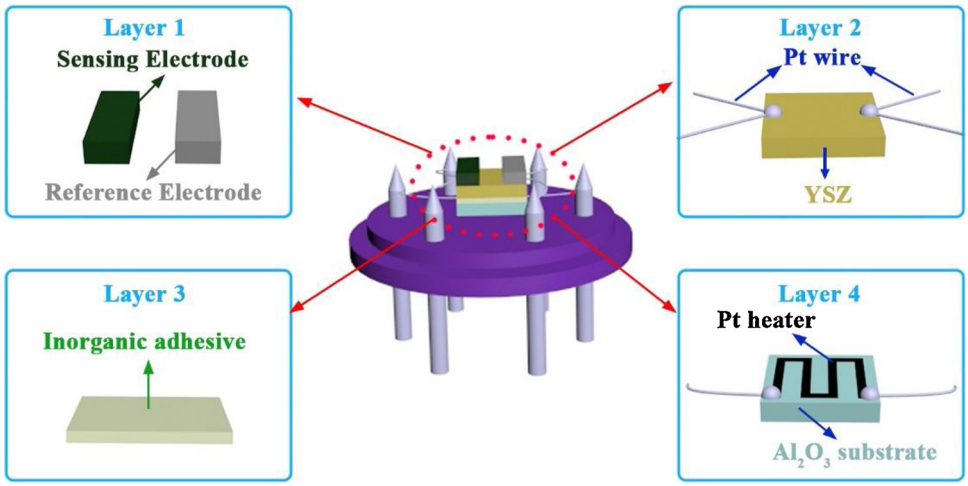

Fig. 1. The schematic structure diagram of the fabricated sensor.

improvement of response/recovery time and the long-term stability. At present, the efforts for improving the performance of sensor mainly focus on choosing and designing novel sensing electrode materials. Co_2SnO_4 is an inverse spinel ternary compound, in which the half of the cobalt ions occupy the octahedral sites and the other half occupy the tetrahedral sites, it has been applied to manufacture lithium ion batteries [19–21] and supercapacitors [22,23] as an outstanding electrode material. It possesses the characteristics of nontoxic and good thermal stability. However, the possibility of Co_2SnO_4 be applied to gas sensing is rarely studied. Therefore, it is feasible to design a YSZ-based gas sensor with a Co_2SnO_4 sensing electrode material and investigate the sensing signal of device toward the target gas.

This is the first time we develop the YSZ-based mixed-potential H_2S sensor utilizing inverse spinel structure Co_2SnO_4-SE synthesized by hydrothermal method. In this work, the H_2S sensing performances of the gas sensor have been measured and investigated in detail. Meanwhile, the probable sensing mechanism of the gas sensor towards H_2S has been systematically proposed and discussed. Furthermore, by simulating and analyzing the exhaled breath detection of healthy people and halitosis patients, we found that the present sensor has a great application prospect in medical diagnosis and treatment.

2. Experimental

2.1. Synthesis of the Co_2SnO_4 sensing electrode material

The Co_2SnO_4 sensing material was synthesized by a simple hydrothermal method. The required raw materials were cobalt chloride hexahydrate ($CoCl_2{\cdot}6H_2O$), stannic chloride pentahydrate ($SnCl_4{\cdot}5H_2O$), cetyl trimethyl ammonium bromide (CTAB), and sodium hydroxide (NaOH) with analytic grade purity, and they were purchased from commercial approach. The detailed progress of preparation was as follows. Firstly, 2 mmol $CoCl_2{\cdot}6H_2O$ was dissolved in 40 mL deionized water to form homogeneous solution, and kept stirring at the room temperature. Then, 1 mmol $SnCl_4{\cdot}5H_2O$, 0.2 g CTAB and 0.03 mol NaOH were orderly added into the above solution every 10 min to form mixed solution. After 15 min of magnetic stirring, the mixed solution was transferred into a Teflon-lined stainless steel autoclave of 50 mL, and reacted at 180 °C for 12 h. Subsequently, the precipitates of cooling to room temperature were centrifuged and washed with deionized water and ethanol several times, then dried in the vacuum oven of 80 °C for 24 h to obtain the precursor. Finally, the precursor material was annealed at 1000 °C for 3 h with a heating rate of 5 °C/min to get the Co_2SnO_4 sensing electrode material.

2.2. Characterization of the Co_2SnO_4 sensing electrode material

The X-ray diffraction (XRD) pattern of Co_2SnO_4 was acquired using Rigaku wide-angle X-ray diffractometor (D/max rA, Cu Kα radiation, wave length $\lambda = 0.15418$ nm) with $5-85^{\circ}$ angular range. The morphology of Co_2SnO_4 material was characterized via a JEOL JSM-7500 F Field-emission scanning electron microscopy (FESEM) of accelerating voltage = 15 kV. Transmission electron (TEM), high-resolution transmission electron microscopy (HRTEM) and the energy dispersive X-ray spectrometry (EDS) were measured by a JEM-2200FS apparatus (JEOL) operating at 200 kV. The Raman spectroscopy of the Co_2SnO_4-SE material was obtained using LabRAM HR Evolution spectrometer (excitation wavelength $\lambda_{ex} = 473$ nm).

2.3. Fabrication and measurement of the gas sensor

YSZ plate (8 mol% Y_2O_3-doped, 2 mm × 2 mm square, 0.3 mm thickness, offered by Anpeisheng Corp. China) was used as solid electrolyte of the gas sensor. The detailed fabrication process was as follows. Firstly, the commercial Pt paste (Sino-platinum Metals Co., Ltd.) was brushed on one side of the YSZ plate to form a narrow Pt stripe, meanwhile, the other side of the YSZ plate was brushed with a Pt point. Then the above-obtained substrate was sintered at 1000 °C for 0.5 h to get Pt reference electrode (RE). Secondly, the sensing electrode paste which was obtained by mixing the Co_2SnO_4 sensing material and a little amount of deionized water was coated on the Pt point to form the stripe-shaped sensing electrode (SE). Whereafter, the device was calcined at 800 °C for 2 h that could form compact contact between YSZ solid electrolyte and Co_2SnO_4-SE. Finally, the Al_2O_3 substrate with Pt heater was glued on the back of the YSZ plate with an inorganic adhesive (formed by the sodium silicate ($Na_2SiO_3{\cdot}9H_2O$) and Al_2O_3 powder) which can provide operating temperature for the sensor. The schematic diagram of prepared YSZ-based gas sensor was exhibited in Fig. 1, and from top to bottom are presented by Layer 1 - Layer 4, respectively. The gas sensing characteristics of the fabricated sensor with Co_2SnO_4-SE were investigated by a traditional static method [24]. Approximately 100 ppm of the H_2S standard gas (Changchun Juyang Gas Co., Ltd) was used to gain different concentrations of H_2S test gases by diluting with air in a 1 L measurement chamber. The gas sensing response value, which was defined as potential difference ($\Delta V = V_{gas} - V_{air}$), was measured by a digital electrometer (Rigol Technologies, Inc., DM3054, China) and the data were synchronously saved in the computer that connecting with the electrometer. Besides, during the gas testing process, for better keeping the accuracy and preciseness of the ΔV of the gas sensor, the measurement times of sensor in each of air and tested gas were strictly controlled by 3 min and 2 min, respectively. The

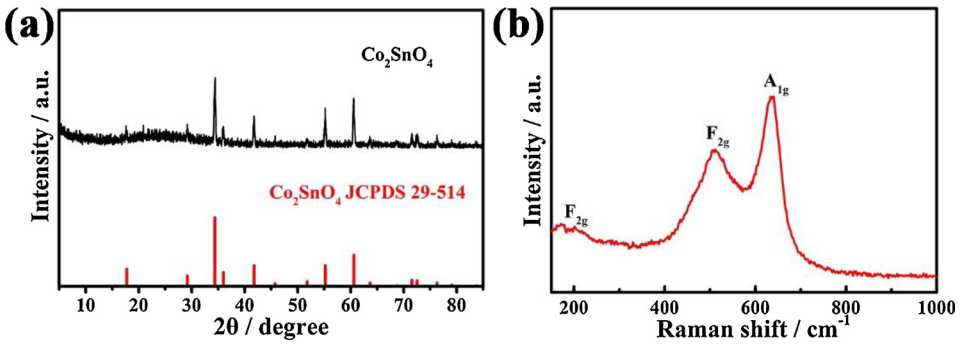

Fig. 2. (a) XRD pattern and (b) Raman spectrum of Co_2SnO_4 sensing material sintered at 1000 °C.

V_{gas} and V_{air} were the potential value when the sensor exposed in the tested gas and in the air at the last second, respectively. The impedance analyzer (Solartron 1260 and Solartron 1287) with the frequency range of 1 MHz-0.1 Hz was used for performing the complex impedance of the sensor in various gases. The current-voltage (polarization) curves of the Co_2SnO_4-SE sensor were tested by the potentiodynamic method (CHI 600C, Instrument corporation of Shanghai, China) in the air, 500 ppb and 1 ppm H_2S sample gases. The tested gases under different relative humidity (RH) were prepared through the humidity chamber (Shanghai ESPC Environment Equipment Corporation, China) at 22 °C. As the simulating halitosis detection method used in the reported works [25–27], the exhaled breathes were collected from the healthy people, and the measurement of simulating halitosis was carried out via injecting the exhaled breath of the healthy people and 1 ppm H_2S into 1 L measurement chamber.

3. Results and discussion

The relevant crystalline structure information of the as-synthesized Co_2SnO_4 sensing material was determined by the XRD pattern. As shown in Fig. 2(a), every diffraction peak of the Co_2SnO_4 sample can be indexed and well correspond to the diffraction peaks in standard card JCPDS No. 29-514. No impurity peaks were observed, which illustrated the pure cubic phase Co_2SnO_4 was obtained. Besides, all sharp and narrow peaks indicated the synthetic product possessed the high crystallinity. Fig. 2(b) exhibited the Raman spectrum of the Co_2SnO_4 sample, the location of the intensity peak mainly appeared at 509 and 637 cm^{-1} due to the F_{2g} and A_{1g} vibrational modes, which were close to the values reported in the literatures [28,29]. SEM was used to observe the surface morphology of the material and the contact condition between the material and the solid electrolyte. From Fig. 3(a and b), after the high temperature calcination of 1000 °C, the Co_2SnO_4 sensing material was composed of particles aggregated together and part cube structure. Such unique structure forms porous channels for rapid diffusion of the gas molecules. The cross-section image of SEM displayed that the sensing electrode layer was about 71.3 μm in thickness, and it was evenly and tightly covered on the surface of YSZ solid electrolyte, which manifests a good contact between SE and YSZ. TEM images of Fig. 4(a and b) clearly showed that the Co_2SnO_4 sensing material was comprised of nano-scale particles and cube structure with a size of about 1.5 μm. The HRTEM images can provide the information of lattice structure in detail. From the two insets of the Fig. 4(c and d), (311) and (222) lattice plane of Co_2SnO_4 can be identified with the lattice fringe spacing of 0.26 nm and 0.25 nm, respectively. Moreover, in EDS mapping results of Fig. 4(e–h), the three elements of Co, O and Sn were uniformly distributed in the Co_2SnO_4.

Generally, the response value of solid state electrolyte sensor was correlative with the operating temperature. Hence, the gas sensing influence of the operating temperature of the device to 1 ppm H_2S was investigated in the temperature range of 460 − 560 °C. As shown in Fig. 5(a), the fabricated gas sensor attached with Co_2SnO_4-SE had the highest response value to 1 ppm H_2S at 510 °C, however, below or above this temperature, the response descended. This phenomenon can be explained as follows: The activation energy required to participate in the electrochemical reaction increases with the increase of temperature. When the temperature exceeded 510 °C, the increase of temperature made that the desorption process of gas plays a major role on the sensing electrode. Therefore, 510 °C can be recognized as the optimal operating temperature of the fabricated sensor, and subsequent gas sensing measurements are performed at 510 °C.

A good continuous dynamic response-recovery curves can reflect the good sensing performance of the sensor. Fig. 5(b) exactly displayed the response and recovery performances of the prepared sensor with Co_2SnO_4-SE in various H_2S concentration atmosphere at 510 °C. Obviously, in the concentration range of 0.1 − 10 ppm H_2S, the response value of sensor augmented synchronously with the increasing of H_2S concentration. Moreover, the fabricated sensor attached with Co_2SnO_4-SE displayed the low detection limit of 100 ppb with the response value of −2.5 mV, indicating that the sensor can effectively detect the low concentration of H_2S from human exhaled breath. Thereby the sensor exhibited the possibility of being a promising candidate for the diagnosis of halitosis. Additionally, the response signal could reach stable

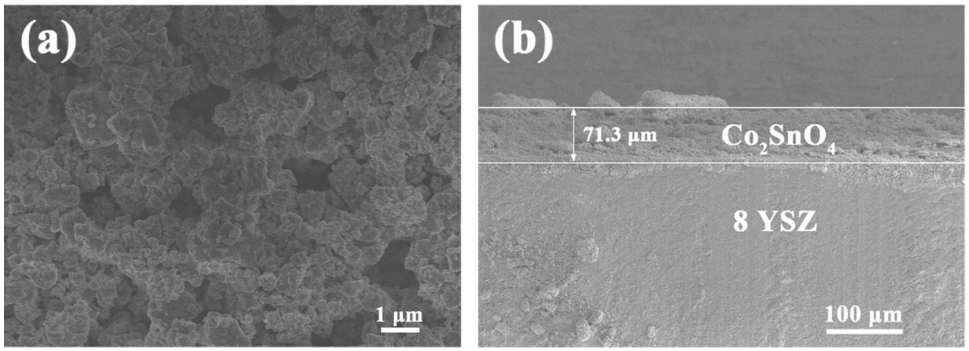

Fig. 3. (a) Surface SEM image and (b) Cross-section SEM image of Co_2SnO_4-SE.

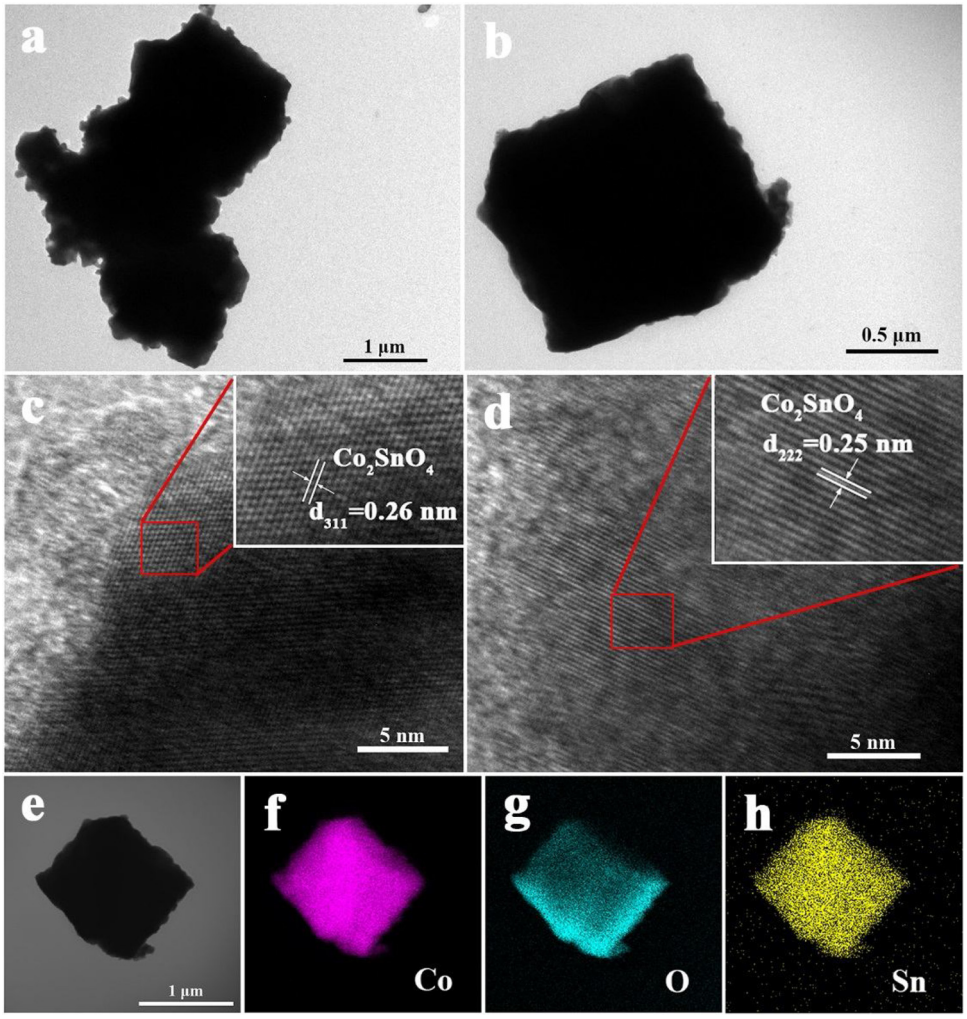

Fig. 4. (a, b) Low magnification and (c, d) HRTEM images of Co_2SnO_4 sensing material sintered at 1000 °C; (e–h) TEM image of Co_2SnO_4-SE and the corresponding EDS mapping images of Co, O, Sn.

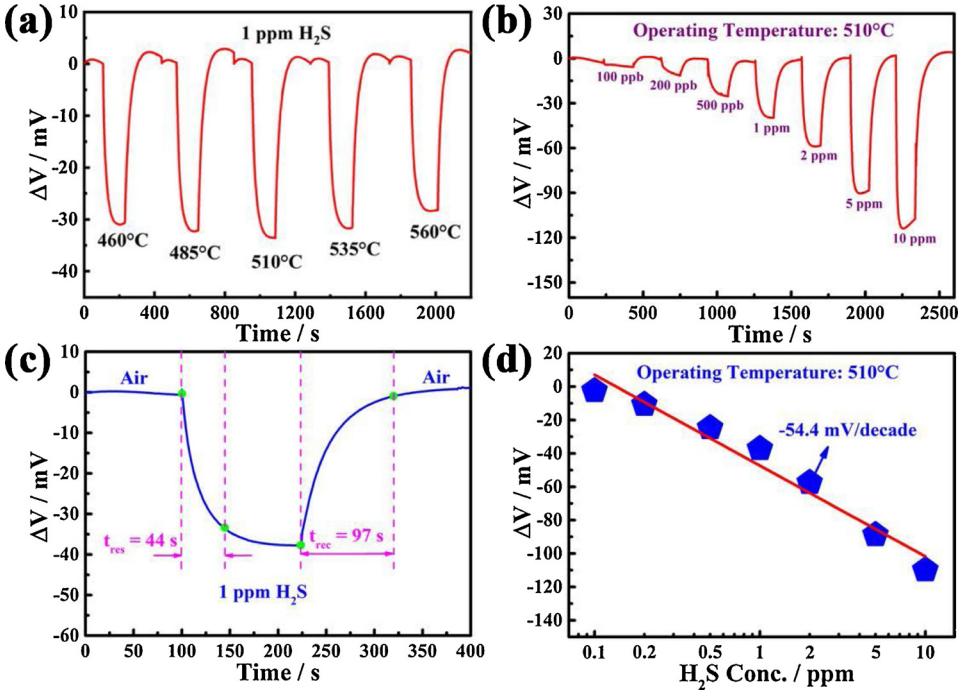

Fig. 5. (a) The response and recovery curves of the sensor attached with Co_2SnO_4-SE to 1 ppm H_2S at different operating temperatures; (b) Response transients of the sensor to different concentrations of H_2S in the range of 0.1-10 ppm at 510 °C; (c) Response and recovery times of the sensor using Co_2SnO_4-SE to 1 ppm H_2S; (d) Dependence of ΔV for the prepared sensor on the logarithm of H_2S concentration in the range of 0.1-10 ppm at 510 °C.

Table 1
Comparison of the sensing performance based on different gas sensors to H_2S.

Sensor Type	Material of AB_2O_4 structure	H_2S Conc. (ppm)	Response	Response/Recovery times (s)	Detection range of H_2S (ppm)	Ref.
Semiconductor	PI-ZFO	1	4.5 ($S = R_a/R_g$)	8/20	1 – 100	[41]
Semiconductor	$CuFe_2O_4$	25	~0.3 ($S = R_a/R_g$)	32±10/-	10 – 300	[42]
Semiconductor	$ZnCo_2O_4$	5	6.27 ($S = R_g/R_a$)	35/-	0.1 – 50	[43]
NASICON	$CoCr_{1.2}Mn_{0.8}O_4$	1	100 mV	< 100/ < 100	0.1 – 20	[15]
YSZ	$NiMn_2O_4$	1	−148 mV	300/275	0.05 – 2	[17]
YSZ	La_2NiO_4	0.5	−55 mV	72/1200	0.02 – 2	[18]
YSZ	Co_2SnO_4	1	−37.2 mV	44/97	0.1 – 10	This work

state in a short time (less than 1.5 min) when the sensor placed in the low concentration range of 0.1 – 5 ppm H_2S. That's because at low concentration H_2S, the quantities of active sites for accelerating electrochemical reaction were enough, resulting in the response amplitude of the sensor depends on the concentration of the target gas. Nevertheless, the response value of the sensor to 10 ppm H_2S began to appear the trend of diminution, the probable reason lied in that partial active site of three phase boundary (TPB, the interface of Co_2SnO_4-SE, YSZ and H_2S) were occupied and the desorption of H_2S gas molecules from the SE material. More importantly and interestingly, the response and recovery times of 44 s and 97 s in 1 ppm H_2S showed the sensor has capacity of realizing rapid detection of H_2S (Fig. 5(c)). Compared with other sensors with AB_2O_4 structure as sensing electrode that have been reported in Table 1, the present sensor attached with Co_2SnO_4-SE in this work showed the fastest response and recovery rates and a relatively good sensing properties. By fitting curve in Fig. 5(d), it can be found that this was a negative linear correlation between the response value of the sensor and the logarithm of H_2S concentration within the range of 0.1 – 10 ppm at 510 °C with the sensitivity of -54.4 mV/decade.

The sensing characteristics of the YSZ-based sensor attached with Co_2SnO_4-SE could be constructed by the mixed potential sensing mechanism. As reported in the literatures [30,31], the solid electrolyte sensor based on oxygen ions conducting electricity can be regarded as an electrochemical cell.

In air: O_2, Co_2SnO_4 / YSZ / Pt, O_2

In sample gas: $H_2S + O_2$, Co_2SnO_4 / YSZ / Pt, $H_2S + O_2$

The electrochemical cathodic reaction (1) and the anodic reaction (2) simultaneously took place on the TPB consisting of Co_2SnO_4-SE, YSZ and H_2S gas. A mixed potential V_M can be obtained on the sensing electrode when the rates of these two reactions arrive at a state of dynamic equilibrium.

$$\text{Cathodic reaction: } O_2 + 4e^- \rightarrow 2O^{2-} \quad (1)$$

$$\text{Anodic reaction: } 2/3H_2S + 2O^{2-} \rightarrow 2/3SO_2 + 2/3H_2O + 4e^- \quad (2)$$

The expression of V_M can be listed by Eq. (3), which was gained by the quantitatively derivation of Butler-Volmer Equation [32,33].

$$V_M = V_0 + mA \ln C_{O_2} - nA \ln C_{H_2S} \quad (3)$$

Where V_0, m, n and A are constants. When the concentration of O_2 (C_{O_2}) was settled, the Eq. (3) could be converted to Eq. (4).

$$V_M = V_0 - nA \ln C_{H_2S} \quad (4)$$

From the above analyses, it was accorded with the experimental result exhibited in Fig. 5(d), which exactly proved the mixed potential theory that the ΔV of the sensor coupled with Co_2SnO_4-SE varied linearly with the concentration logarithm of H_2S.

Fig. 6 showed the response and recovery curves of the sensor to 1 ppm H_2S in eight cycles testing. The potential difference value in eight measurement cycles were almost equal and the response-recovery curves of every cycle could be repeatable well. Therefore, it can be considered that the sensor with Co_2SnO_4-SE possessed the nature of good reproducibility. The humidity resistance has always been one of the most important factors of solid state electrolyte sensor, especially

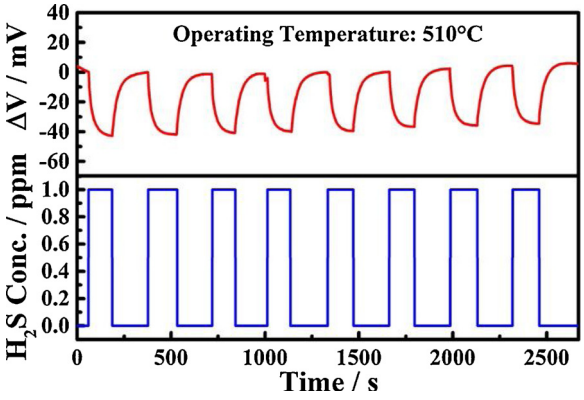

Fig. 6. Continuous response and recovery curves of the sensor attached with Co_2SnO_4-SE to 1 ppm H_2S at the operating temperature of 510 °C.

the exhaled gas from the human body also contains a large amount of water vapor. Thus, it's essential to estimate the effect of humidity to the sensing performance of the sensor. As displayed in Fig. 7(a and b), the response values of the sensor displayed a fluctuation within a narrow range with increase of relative humidity. Although the gas sensing performance had some attenuation in resisting humidity, the sensor based on the Co_2SnO_4-SE was still considered as a promising device to detect H_2S for its receivable and stable response signal at high 80 % even 98 % RH.

As is known to all, the exhaled gas not only contains a mass of water vapor, but also includes a variety of coexist gases. Therefore, the selectivity of the sensor to H_2S was evaluated by testing the cross-sensitivity to some interfering gases. Fig. 8(a) depicted that the ΔV of the sensor attached with Co_2SnO_4-SE to the different concentrations of other interfering gases were much lower than that of 1 ppm H_2S at 510 °C. In addition, the gas mixtures of 1 ppm H_2S and different concentrations of interfering gases were prepared to further investigate the cross-sensitivity property of the sensor in Fig. 8(b). The result showed that comparing with the response value of 1 ppm pure H_2S, the fluctuating values in the mixed gases atmosphere changed at the range of 0.4 mV to -12.8 mV. Hence, the sensor coupled with Co_2SnO_4-SE has the good selectivity to H_2S among kinds of interference gases.

To make clearly the reason that the selectivity of the sensor to H_2S, the impedance measurement had been carried out and exhibited in Fig. 9(a). According to the previously reported literatures [34,35], the total resistance was mainly affected by the interfacial resistance between YSZ and sensing electrode. The interfacial resistance can be given by the intersection of the large semi-arc and the real axis at the lower frequency range (around 0.1 Hz). The lower the resistance value, the higher the catalytic activity of electrochemical reaction. Here, the resistances were almost no change at the high frequency range, however, at lower frequency (about 0.1 Hz), the resistance value of other gases (CO, C_2H_2, NH_3, CO_2) were augmented comparing with H_2S gas. This phenomenon represented the highest electrochemical catalytic activity of Co_2SnO_4 sensing material towards H_2S. Consequently, the gas sensor attached with Co_2SnO_4-SE possessed best sensing performance to H_2S at

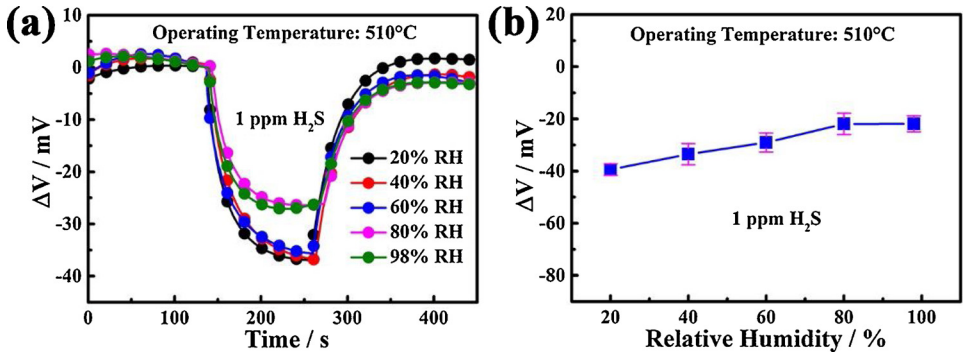

Fig. 7. (a, b) The influence of different relative humidity on sensing signal of the sensor to 1 ppm H_2S at 510 °C (Different relative humidity were obtained in a humidity chamber at 22 °C).

510 °C. Based on the reported literatures [36–40], a probably equivalent circuit was given for the fabricated sensor attached with Co_2SnO_4-SE. Here, R_0 represents the total impedance of wires and solid electrolyte, R_{se} and C_{se} are impedance and capacitance of the oxide sensing electrode respectively, representing the first semi-circle at the high frequency range, which is related to nature of itself, isn't affected by test gas. R_{ct} and C_{ct} represent the impedance and capacitance of the interface between YSZ and sensing electrode, respectively, and the interface impedance value (R_{ct}) reflects the degree of electrochemical reaction at the interface. Besides, for verifying the fabricated sensor abided the mixed potential mechanism, the polarization curves were tested in air, 500 ppb H_2S and 1 ppm H_2S by the linear sweep voltammetry. As the results revealed in Fig. 9(b), the cathodic polarization curve was measured in air, and the anodic polarization curves were gained by subtracting in air from in different concentrations of H_2S. The intersection of anodic and cathodic polarization curve was the mixed-potential estimated value of the fabricated sensor. Apparently, the experimental observed value in 500 ppb (−24.7 mV) and 1 ppm H_2S (−37.2 mV) were close to the estimated values (-25.8 and -37.5 mV). What's more, the anodic polarization curve in high concentration toward left to reach higher potential, which was consistent with Eq. (4). Above results illustrated the present sensor using Co_2SnO_4-SE calcined at 1000 °C was following the mixed potential theory.

To evaluate the potential application value of the sensor attached with Co_2SnO_4-SE in the detection of halitosis, the simulation test environment was prepared via collecting the exhaled breath of healthy groups and halitosis patients (simulated by injecting 1 ppm H_2S to the healthy exhaled breath). Here, the concentration of H_2S was selected as 1 ppm because the content of H_2S more than 0.1 ppm in exhaled breath can be regarded as halitosis patient [8]. Fig. 10 showed the responses of sensor in health and simulating halitosis breath of ten volunteers. Obviously, the response values of the sensor toward health breath chiefly focused at the range of −14 mV to −7 mV. However, when the sensor exposed to the gas mixture of the simulated halitosis patients, the response values mainly gathered at the range of −52.5 mV to −40 mV. The difference in ΔV between healthy and halitosis subjects was notable. Therefore, the fabricated sensor performed good prospect in halitosis diagnose by distinguishing H_2S from human exhaled breath.

The good stability of the gas sensor is a prerequisite for continuously operating at high temperatures. For this purpose, the response data of present sensor to 1 ppm H_2S in 31 days were recorded and showed in Fig. 11(a). It was clearly that the variation of ΔV was tiny, additionally, which can be observed by the ΔV_s. The formula of ΔV_s is defined as:

$$\Delta V_s = [(\Delta V_n - \Delta V_0)] / \Delta V_0 \times 100\ \% \quad (5)$$

Where ΔV_0 and ΔV_n represent the response value of the sensor on the initial and nth day, respectively. After the consecutive measurement in 31 days, the attenuation amplitude was less than -14 %. Furthermore, Fig. 11(b) exhibited the response and recovery curves of the sensor to 1 ppm H_2S on the initial, 16th, 31th day, which indicated the sensor based on Co_2SnO_4-SE could continuously detect the H_2S at high temperature. Thus, the prepared sensor maintained good sensing performance during the consecutive 31-day measurement period and possessed good long-term stability.

4. Conclusion

The Co_2SnO_4 with spinel structure was initially used as sensing electrode to fabricate YSZ-based H_2S sensor. The Co_2SnO_4 sensing material was synthesized via hydrothermal method and the characterization results of XRD, Raman, SEM, TEM, HRTEM and EDS clearly proved the crystal structure of pure phase formed at the calcination temperature of 1000 °C. In the respect of gas sensing performance, the YSZ-based H_2S sensor attached with Co_2SnO_4-SE displayed rapid response time of 44 s in 1 ppm H_2S, as well as high sensitivity of −54.4 mV/decade to 0.1−10 ppm H_2S at 510 °C and low detection

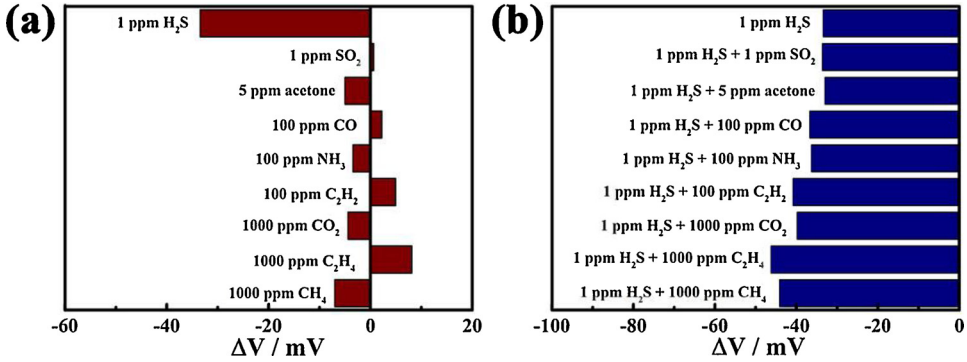

Fig. 8. (a) The responses of the fabricated sensor attached with Co_2SnO_4-SE to various gases at 510 °C; (b) The cross-sensitivities of the sensor to gas mixture (1 ppm H_2S and other interference gases) at 510 °C.

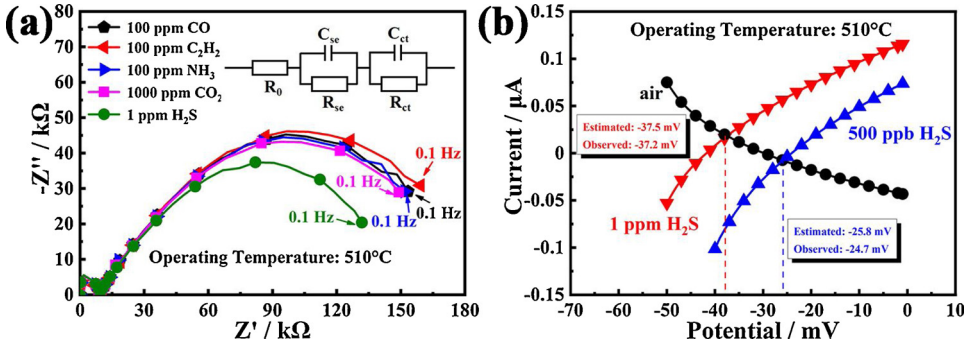

Fig. 9. (a) Impedance curves of the present sensor attached with Co_2SnO_4-SE in the gases of CO, C_2H_2, NH_3, CO_2, H_2S at 510 °C; (b) Polarization curves of the sensor in air and different concentrations of H_2S at 510 °C.

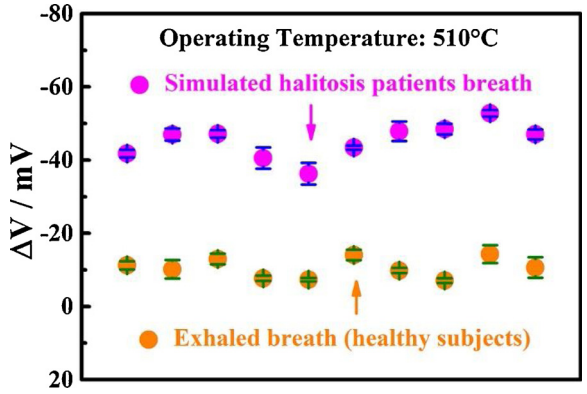

Fig. 10. The recognition of the fabricated sensor based on Co_2SnO_4-SE to human exhaled breath (healthy subjects and simulated halitosis patients) at 510 °C.

limit of 100 ppb H_2S. The prepared sensor also possessed good reproducibility, selectivity, acceptable humidity resistance and good long-term stability. More importantly, the fabricated sensor displayed the visible response difference between the exhaled breath from 10 healthy people and the simulated halitosis breath. Hereto, the presented sensor utilizing Co_2SnO_4-SE provided a feasible method for H_2S detection and it has great development prospect in the field of halitosis monitoring.

CRediT authorship contribution statement

Caileng Wang: Investigation, Methodology, Data curation, Formal analysis, Software, Writing - original draft, Writing - review & editing. **Li Jiang:** Methodology, Data curation, Software, Writing - review & editing. **Jing Wang:** Methodology, Writing - review & editing. **Fangmeng Liu:** Methodology, Formal analysis, Supervision, Writing - review & editing. **Rui You:** Methodology, Writing - review & editing. **Siyuan Lv:** Methodology, Writing - review & editing. **Zijie Yang:** Methodology, Writing - review & editing. **Junming He:** Methodology, Writing - review & editing. **Ao Liu:** Methodology, Writing - review & editing. **Xu Yan:** Methodology, Writing - review & editing. **Chenguang Wang:** Methodology, Writing - review & editing. **Peng Sun:** Methodology, Writing - review & editing. **Xishuang Liang:** Methodology, Writing - review & editing. **Geyu Lu:** Methodology, Funding acquisition, Supervision, Writing - review & editing.

Declaration of Competing Interest

The authors declare that they have no known competing financial interests or personal relationships that could have appeared to influence the work reported in this paper.

Acknowledgements

This work is supported by the National Nature Science Foundation of China (Nos. 61831011, 61803171, 61520106003, 61722305 and 61833006), Program for Chang Jiang Scholars and Innovative Research Team in University (No. IRT-17R47), National Key Research and Development Program of China (Nos. 2016YFC0207300 and 2016YFC0201002), Application and Basic Research of Jilin Province (20130102010 JC), Young Elite Scientists Sponsorship Program by CAST (2018QN RC001), Program for JLU Science and Technology Innovative Research Team (JLUSTIRT 2017TD-07), China Postdoctoral Science Foundation Funded Project (No. 2018M630322, 2019T120239), Jilin Provincial Science and Technology Development Program (20190103155JH), Jilin Provincial Education Department Science and Technology Project (JJKH20190114KJ), Fundamental Research Funds for the Central Universities.

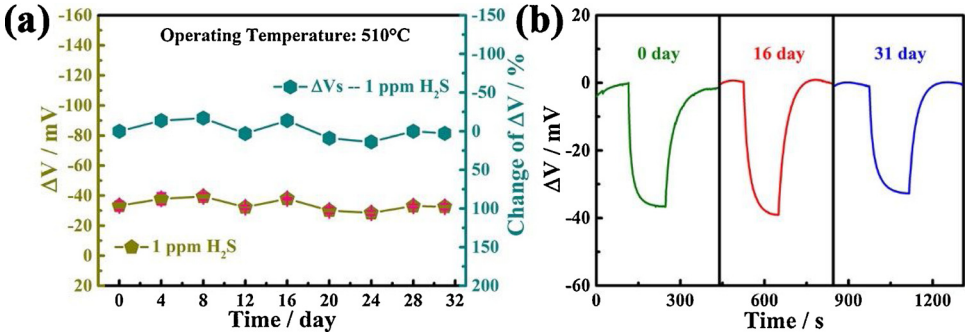

Fig. 11. (a) Long-term stability of the sensor attached with Co_2SnO_4-SE to 1 ppm H_2S; (b) The response and recovery curves of the sensor to 1 ppm H_2S on the initial, 16th, 31th day at 510 °C.

References

[1] C. Bollen, T. Beikler, Halitosis: the multidisciplinary approach, Int. J. Oral Sci. 4 (2012) 55–63.
[2] A. da Mota, C. Franca, R. Prates, A. Deana, L. Santos, R. Garcia, M. Goncalves, R. Mesquita-Ferrari, K. Fernandes, S. Bussadori, Effect of photodynamic therapy for the treatment of halitosis in adolescents-a controlled, microbiological, clinical trial, J. Biophotonics 9 (2016) 1337–1343.
[3] U. Kandalam, N. Ledra, H. Laubach, K. Venkatachalam, Inhibition of methionine gamma lyase deaminase and the growth of Porphyromonas gingivalis: a therapeutic target for halitosis/periodontitis, Arch. Oral Biol. 90 (2018) 27–32.
[4] S. Porter, C. Scully, Oral malodour (halitosis), Br. Med. J. 333 (2006) 632–635.
[5] J. Tonzetich, Production and origin of oral malodor: a review of mechanisms and methods of analysis, J. Periodont. 48 (1977) 13–20.
[6] G. Delanghe, J. Ghyselen, D. van Steenberghe, L. Feenstra, Multidisciplinary breath-odour clinic, Lancet 350 (1997) 187.
[7] A. Tangerman, Halitosis in medicine: a review, Int. Dent. J. 52 (2002) 201–206.
[8] K. Choi, H. Kim, Y. Kang, J. Lee, Ultraselective and ultrasensitive detection of H_2S in highly humid atmosphere using CuO-loaded SnO_2 hollow spheres for real-time diagnosis of halitosis, Sens. Actuators B Chem. 194 (2014) 371–376.
[9] Y. Shimizua, H. Nakanoa, S. Takasea, J. Song, Solid electrolyte impedancemetric NO_x sensor attached with zeolite receptor, Sens. Actuators B Chem. 264 (2018) 177–183.
[10] M. Mori, Y. Itagaki, Y. Sadaoka, S. Nakagawa, M. Kida, T. Kojima, Detection of offensive odorant in air with a planar-type Potentiometric gas sensor based on YSZ with Au and Pt electrodes, Sens. Actuators B Chem. 191 (2014) 351–355.
[11] X. Liang, G. Lu, T. Zhong, F. Liu, B. Quan, New type of ammonia/toluene sensor combining NASICON with a couple of oxide Electrodes, Sens. Actuators B Chem. 150 (2010) 355–359.
[12] T. Nagai, S. Tamura, N. Imanaka, Solid electrolyte type ammonia gas sensor based on trivalent aluminum ion conducting solids, Sens. Actuators B Chem. 147 (2010) 735–740.
[13] L. Dai, H. Zhou, G. Yang, Y. Li, J. Zhu, L. Wang, Ammonia sensing characteristics of $La_{10}Si_5MgO_{26}$-based amperometric-type sensor attached with nano-structured $CoWO_4$ sensing electrode, J. Alloys. Compd. 663 (2016) 86–93.
[14] X. Liang, Y. He, F. Liu, B. Wang, T. Zhong, B. Quan, G. Lu, Solid-state potentiometric H_2S sensor combining NASICON with Pr_6O_{11}-doped SnO_2 electrode, Sens. Actuators B Chem. 125 (2007) 544–549.
[15] H. Zhang, T. Zhong, R. Sun, X. Liang, G. Lu, Sub-ppm H_2S sensor based on NASICON and $CoCr_{2-x}Mn_xO_4$ sensing electrode, RSC Adv. 4 (2014) 55334–55340.
[16] N. Miura, Y. Yan, G. Lu, N. Yamazoe, Sensing characteristics and mechanism of hydrogen sulfide sensor using stabilized zirconia and oxide sensing electrode, Sens. Actuators B Chem. 34 (1996) 367–372.
[17] Y. Guan, C. Yin, X. Cheng, X. Liang, Q. Diao, H. Zhang, G. Lu, Sub-ppm H_2S sensor based on YSZ and hollow balls $NiMn_2O_4$ sensing electrode, Sens. Actuators B Chem. 193 (2014) 501–508.
[18] X. Hao, C. Ma, X. Yang, T. Liu, B. Wang, F. Liu, X. Liang, C. Yang, H. Zhu, G. Lu, YSZ-based mixed potential H_2S sensor using La_2NiO_4 sensing electrode, Sens. Actuators B Chem. 255 (2018) 3033–3039.
[19] B. Wang, J. Zhang, Z. Xia, K. Shu, Facile synthesis of graphene encapsulated Co_2SnO_4 nanoparticles as enhanced anode materials for lithium-ion batteries, J. Nanosci. Nanotechnol. 18 (2018) 5679–5685.
[20] J. Zhang, J. Liang, Y. Zhu, D. Wei, L. Fan, Y. Qian, Synthesis of $Co2SnO_4$ hollow cubes encapsulated in graphene as high capacity anode materials for lithium-ion batteries, J. Mater. Chem. A 2 (2014) 2728–2734.
[21] C. Chen, Q. Ru, S. Hu, B. An, X. Song, X. Hou, Co_2SnO_4 nanocrystals anchored on graphene sheets as high-performance electrodes for lithium-ion batteries, Electrochim. Acta 151 (2015) 203–213.
[22] B. Gnana Sundara Raj, S. Bhuvaneshwari, J. Wu, A. Asiri, S. Anandan, Sonochemical synthesis of Co_2SnO_4 nanocubes for supercapacitor applications, Ultrason. Sonochem. 41 (2018) 435–440.
[23] P. He, Z. Xie, Y. Chen, F. Dong, H. Liu, Co_2SnO_4/activated carbon composite electrode for supercapacitor, Mater. Chem. Phys. 137 (2012) 576–579.
[24] C. Wang, X. Cheng, X. Zhou, P. Sun, X. Hu, K. Shimanoe, G. Lu, N. Yamazoe, Hierarchical α-Fe_2O_3/NiO composites with a hollow structure for a gas sensor, ACS Appl. Mater. Interfaces 6 (2014) 12031–12037.
[25] W. Liu, J. Sun, L. Xu, S. Zhu, X. Zhou, S. Yang, B. Dong, X. Bai, G. Lu, H. Song, Understanding the noble metal modifying effect on In_2O_3 nanowires: highly sensitive and selective gas sensors for potential early screening of multiple diseases, Nanoscale Horiz. 4 (2019) 1361–1371.
[26] S. Kim, S. Choi, J. Jang, H. Cho, W. Koo, H. Tuller, I. Kim, Exceptional high-performance of Pt-Based bimetallic catalysts for exclusive detection of exhaled biomarkers, Adv. Mater. 29 (2017) 1700737.
[27] G. Pennazza, E. Marchetti, M. Santonico, G. Mantini, S. Mummolo, G. Marzo, R. Paolesse, A. D'Amico, C. Natale, Application of a quartz microbalance based gas sensor array for the study of halitosis, J. Breath Res. 2 (2008) 017009.
[28] M. Ali, A. Barras, A. Addad, B. Sieber, H. Elhouichet, M. Férid, S. Szunerits, R. Boukherroub, Co_2SnO_4 nanoparticles as a high performance catalyst for oxidative degradation of rhodamine B dye and pentachlorophenol by activation of peroxymonosulfate, Phys. Chem. Chem. Phys. 19 (2017) 6569–6578.
[29] M. Bouchard, A. Gambardella, Raman microscopy study of synthetic cobalt blue spinels used in the field of art, J. Raman Spectrosc. 41 (2010) 1477–1485.
[30] X. Hao, B. Wang, C. Ma, F. Liu, X. Yang, T. Liu, X. Liang, C. Yang, H. Zhu, G. Lu, Mixed potential type sensor based on stabilized zirconia and $Co_{1-x}Zn_xFe_2O_4$ sensing electrode for detection of acetone, Sens. Actuators B Chem. 255 (2018) 1173–1181.
[31] F. Liu, J. He, Z. Yang, R. You, J. Wang, L. Zhao, Q. Wang, X. Liang, P. Sun, X. Yan, G. Lu, The mixed potential type gas sensor based on stabilized zirconia and molybdate $MMoO_4$ (M: Ni, Co and Zn) sensing electrode aiming at detecting trimethylamine, Sens. Actuators B Chem. 267 (2018) 430–437.
[32] J. Wang, A. Liu, C. Wang, R. You, F. Liu, S. Li, Z. Yang, J. He, X. Yan, P. Sun, G. Lu, Solid state electrolyte type gas sensor using stabilized zirconia and $MTiO_3$ (M: Zn, Co and Ni)-SE for detection of low concentration of SO_2, Sens. Actuators B Chem. 296 (2019) 126644.
[33] F. Liu, S. Li, J. He, J. Wang, R. You, Z. Yang, L. Zhao, P. Sun, X. Yan, X. Liang, X. Chuai, G. Lu, Highly selective and stable mixed-potential type gas sensor based on stabilized zirconia and $Cd_2V_2O_7$ sensing electrode for NH_3 detection, Sens. Actuators B Chem. 279 (2019) 213–222.
[34] M. Nakatou, N. Miura, Detection of propene by using new-type impedancemetric zirconia-based sensor attached with oxide sensing-electrode, Sens. Actuators B Chem. 120 (2006) 57–62.
[35] Y. Chen, J. Xiao, Effects of YSZ addition on the response of La_2CuO_4 sensing electrode for a potentiometric NO_X sensor, Sens. Actuators B Chem. 192 (2014) 730–736.
[36] N. Miura, T. Koga, M. Nakatou, P. Elumalai, M. Hasei, Electrochemical NO_x sensors based on stabilized zirconia: comparison of sensing performances of mixed-potential-type and impedancemetric NO_x sensors, J. Electroceram. 17 (2006) 979–986.
[37] M. Stranzenbach, E. Gramckow, B. Saruhan, Planar, impedance-metric NO_x-sensor with spinel-type SE for high temperature applications, Sens. Actuators B Chem. 127 (2007) 224–230.
[38] N. Miura, M. Nakatou, S. Zhuiykov, Impedancemetric gas sensor based on zirconia solid electrolyte and oxide sensing electrode for detecting total NO_x at high temperature, Sens. Actuators B Chem. 93 (2003) 221–228.
[39] K. Cvejin, M. Śliwa, L. Manjakkal, J. Kulawik, G. Stojanović, D. Szwagierczak, Impedancemetric NO sensor based on YSZ/perovskite neodymium cobaltite operating at high temperatures, Sens. Actuators B Chem. 228 (2016) 612–624.
[40] N. Wu, Z. Chen, J. Xu, M. Chyu, S. Mao, Impedance-metric Pt/YSZ/Au-Ga_2O_3 sensor for CO detection at high temperature, Sens. Actuators B Chem. 110 (2005) 49–53.
[41] J. Wu, D. Gao, T. Sun, J. Bi, Y. Zhao, Z. Ning, G. Fan, Z. Xie, Highly selective gas sensing properties of partially inversed spinel zinc ferrite towards H_2S, Sens. Actuators B Chem. 235 (2016) 258–262.
[42] A. Ayesh, M. Haija, A. Shaheen, F. Banat, Spinel ferrite nanoparticles for H_2S gas sensor, Appl. Phys. A-Mater. Sci. Process. 123 (2017) 1–8.
[43] X. Gao, C. Li, C. Zhu, Q. Ouyang, X. Zhang, Y. Chen, Synthesis and low-temperature sensing property of the porous $ZnCo_2O_4$ nanosheets, J. Mater. Sci.-Mater. Electron. 30 (2019) 5357–5365.

Caileng Wang received the B.S. degree in department of electronic science and technology in 2018. She is currently studying for her M.E. Sci. degree in College of Electronic Science and Engineering, Jilin University, China.

Li Jiang received the B.Eng. degree in department of electronic science and technology in 2019. He is currently studying for his M.E. Sci. degree in College of Electronic Science and Engineering, Jilin University, China.

Jing Wang received her B.S. degree in applied chemistry in 2009 and the M.S. degree in polymer chemistry and physics in 2012 from Northeast Forestry University in China. Her current research is solid electrolyte gas sensor.

Fangmeng Liu received his PhD degree in 2017 from College of Electronic Science and Engineering, Jilin University, China. Now he is an associate Professor of Jilin University, China. His current research interests include the application of functional materials and development of solid state electrochemical gas sensor and flexible device.

Rui You received his B.S. degree from Department of Opto-Electronic Engineering in 2013, Changchun University of Science and Technology, Changchun, China. He is now a Ph.D. student at the Department of Precision Instrument at Tsinghua University, Beijing, China. Currently his research interests mainly include gas sensor and application of MEMS process.

Siyuan Lv entered Jilin University in 2016. Now she is studying for her B.Eng. degree in department of electronic science and technology.

Zijie Yang received the B.S. degree in department of electronic science and technology in 2017. He is currently studying for his M.E. Sci. degree in College of Electronic Science and Engineering, Jilin University, China.

Junming He received the B.Eng. degree in department of electronic science and technology in 2017. She is currently studying for her M.E. Sci. degree in College of Electronic Science and Engineering, Jilin University, China.

Ao Liu received the B.Eng. degree in department of electronic science and technology in 2018. He is currently studying for his M.E. Sci. degree in College of Electronic Science and Engineering, Jilin University, China.

Xu Yan received his M.S. degree in 2013 from Nanjing Agricultural University. He joined the group of Prof. Xingguang Su at Jilin University and received his Ph.D. degree in June 2017. Since then, he did postdoctoral work with Prof. Geyu Lu. Currently, his research interests mainly focus on the development of the functional nanomaterials for chem/bio

sensors.

Chenguang Wang received his PhD degree from the College of Chemistry, Jilin University in 2013. He then joined the Institute of Transformative Bio-Molecules, Nagoya University as a postdoctoral fellow. In 2019, he joined the College of Electronic Science and Engineering, Jilin University as a professor. His research interests focus on the design and synthesis of organic fluorescent molecules and their applications in fluorescence bio-imaging.

Peng Sun received his PhD degree from the Electronics Science and Engineering department, Jilin University, China in 2014. Now, he is engaged in the synthesis and characterization of the semiconducting functional materials and gas sensors.

Xishuang Liang received the B. Eng. degree in Department of Electronic Science and Technology in 2004. He received his Doctor's degree in College of Electronic Science and Engineering at Jilin University in 2009. Now he is a professor of Jilin University, China. His current research is solid electrolyte gas sensor.

Geyu Lu received the B.Sci. degree in electronic sciences in 1985 and the M.S. degree in 1988 from Jilin University in China and the Dr. Eng. degree in 1998 from Kyushu University in Japan. Now he is a professor of Jilin University, China. His current research interests include the development of chemical sensors and the application of the function materials.